Challenging zebrafish escape responses by increasing water viscosity

The Journal of Experimental Biology 215, 1854-1862

doi:10.1242/jeb.068957

RESEARCH ARTICLE

Challenging zebrafish escape responses by increasing water viscosity

Nicole Danos* and George V. Lauder

Department of Organismic and Evolutionary Biology, Harvard University, 26 Oxford Street, Cambridge, MA 02138, USA

*Author for correspondence at present address: Ecology and Evolutionary Biology, 321 Steinhaus Hall, University of California Irvine, Irvine, CA 92697, USA (ndanos@post.harvard.edu)

Accepted 8 February 2012

SUMMARY

Escape responses of fishes have long been studied as a model locomotor behavior in which hypothesized maximal or near-maximal muscle power output is used to generate rapid body bending. In this paper we present the results of experiments that challenged zebrafish (*Danio rerio*) to perform escape responses in water of altered viscosity, to better understand the effects that the fluid mechanical environment exerts on kinematics. We quantified escape kinematics using 1000 frames s^{-1} high-speed video, and compared escape response kinematics of fish in three media that differed in viscosity: 1 mPa s (normal water), 10 mPa s and 20 mPa s (20 times normal water viscosity). We hypothesized that because viscosity is increased but not density there will be a different effect on kinematic variables resulting from unsteady (acceleration-dependent) hydrodynamic forces and steady (velocity-dependent) ones. Similarly, we hypothesized that the kinematics of stage 1 will be less affected by viscosity than those of stage 2, as higher angular velocities are reached during stage 1 resulting in higher Reynolds numbers. Our results showed a significant overall effect of viscosity on escape response kinematics but the effect was not in accordance with our predictions. Statistical tests showed that increasing viscosity significantly decreased displacement of the center of mass during stage 1 and after 30 ms, and decreased maximum velocity of the center of mass, maximum angular velocity and acceleration during stage 1, but increased time to maximum angular acceleration and time to maximum linear velocity of the center of mass. Remarkably, increasing water viscosity 20 times did not significantly affect the duration of stage 1 or stage 2.

Key words: locomotion, fish, viscosity, zebrafish.

INTRODUCTION

The escape response of fishes is a widespread model of vertebrate locomotor behavior that has been used to clarify the design of neural circuits (e.g. Eaton et al., 1977; Foreman and Eaton, 1993; Liu and Fetcho, 1999), understand rapid activation of axial muscles (Jayne and Lauder, 1993; Rome et al., 1988; Tytell and Lauder, 2002; Westneat et al., 1998), clarify predator-avoidance dynamics (Walker et al., 2005) and investigate unsteady locomotor hydrodynamics (e.g. Borazjani et al., 2012; Frith and Blake, 1995; Tytell and Lauder, 2008). Escape behavior usually occurs in response to an impulsive hydrodynamic or visual stimulus and is usually (though not always) mediated by the Mauthner cells of the hindbrain (Zottoli, 1977). Escape responses by fishes are characterized by large body angular accelerations and displacements (Domenici and Blake, 1997) and are usually divided into two stages: an initial C-bend (stage 1) and a contralateral bend followed by one or more tailbeats (stage 2).

One assumption that has made escape responses a useful model for studying muscle physiology and mechanics is that this behavior appears to require maximum muscle power production. This is a reasonable assumption given the importance of this behavior in predator avoidance (Walker et al., 2005), although a difficult hypothesis to test directly given the assumptions needed to evaluate the *in vivo* power production of complexly arranged segmental body musculature with multiple fiber types. A number of studies have investigated the power output of fish muscle during escape behaviors and have suggested that the body musculature is activated in a near-maximal manner (e.g. Franklin and Johnston, 1997; Johnston et al., 1995; Wakeling and Johnston, 1998).

One approach that might reveal new features of fish escape response dynamics involves challenging fish to perform their escape behavior under increased loading, i.e. in a more viscous fluid environment. Specifically, we believe that fish induced to perform escape responses in water of substantially higher viscosity than normal should have to increase muscle power output to accomplish normal kinematics in a similar time frame. Alternatively, if muscle power output cannot be increased beyond that seen in normal escape behaviors, then substantial increases in water viscosity (of the order of 20 times normal) might result in longer times for the body to achieve the stage 1 and stage 2 kinematic bending patterns. Increased viscosity should also increase the thickness of the boundary layer around the bending fish and affect body acceleration patterns. Fish might perform the same sequence of kinematic events in water of high viscosity, but each stage could take longer to complete and accelerations might be lower. Altering increased viscosity could also have differential effects on stage 1 and stage 2 of the escape behavior. During stage 2 there are lower accelerations and angular displacements than in stage 1, and this stage is not controlled by the large Mauthner cells with their fast transmission times that activate myotomal muscle fibers (Eaton et al., 1977; Weiss et al., 2006).

Additionally, increased viscosity may also affect C-start kinematics by altering the hydrodynamics that govern fin function. Recent studies have demonstrated the importance of the dorsal and anal fins in producing forces during locomotion in general (Drucker and Lauder, 2005; Standen and Lauder, 2005; Standen and Lauder, 2007) and escape responses in particular (Tytell and Lauder, 2008).

The shedding of vortices from flapping foils is delayed when viscosity is increased (Faber, 1995) and in the case of an accelerating fish this could affect patterns of force production, resulting in different timings of events.

However, the high accelerations and displacements of this locomotor behavior indicate that unsteady forces govern its hydrodynamics, which are poorly understood. But, in addition to the steady-state forces such as skin and pressure drag, hydrodynamic analyses of escape responses need to consider the acceleration reaction force (Daniel, 1984). As the turning fish and its tail accelerate a mass of water, this reaction force acts opposite to the direction of body movement and resists the fish body acceleration. Only water density is expected to affect the magnitude of this force (Daniel, 1984), unless increased viscosity indirectly increases the added mass coefficient.

In this paper, we performed experiments that challenged zebrafish (*Danio rerio*) to perform escape responses in water altered to be 10 and 20 times more viscous than normal water. We found that while increasing water viscosity does have a significant overall effect on the escape response, many of the observed specific changes in C-start kinematics were unexpected, and some variables such as the durations of stages and timing of maximal body bending were not altered.

MATERIALS AND METHODS

Animals and viscosity treatments

Zebrafish, *D. rerio* (Hamilton 1822), were obtained from the Harvard University zebrafish facility and kept in an aquarium under 12 h:12 h light:dark conditions. Five fish were used for the experiments; the experimental design and statistical analyses are described below. Fish (mean total length 33.0±1.3 mm) were placed in a circular container (diameter 12 cm, filled to a depth of 10 cm) with an optically clear base and allowed to swim freely. Video images from below (ventral view) were captured at 1000 frames s^{-1} using a Photron PCI 1024 camera (1024×1024 pixel resolution, Photron Inc., San Diego, CA, USA). A cylindrical object with an added flat base (approximate diameter 1.5 cm) to enhance the initial impact at the water surface was dropped into the tank holding an individual zebrafish to elicit escape responses from the fish. This follows the procedure that we have used in previous experiments on fish escape responses (Jayne and Lauder, 1993; Tytell and Lauder, 2002; Tytell and Lauder, 2008).

Each of the five fish was recorded performing escape responses in media of all three levels of viscosity: 1 mPa s (normal water), 10 mPa s or 20 mPa s. The sequence of viscosity treatments at which each fish was tested was randomized. To prepare high viscosity solutions, Dextran 500 (Pharmacosmos A/S, Holbaek, Denmark) was dissolved in aquarium water. Oxygen levels in the increased viscosity media were monitored using an SM 600 dissolved oxygen meter (Milwaukee Instruments, Rocky Mount, NC, USA) and never fell below 6.5 p.p.m. in any treatment, the equivalent of 84% saturation under our laboratory conditions. Viscosities were measured using shell cup viscometers (Norcross, Newton, MA, USA). Dextran solutions have Newtonian fluid dynamic properties even at the relatively high viscosities used here (Akashi et al., 2000). Newtonian fluids have a constant viscosity, independent of shear stress rate produced by the fish's velocity during the escape response. Although the increased viscosity treatments differed from normal water by an order of magnitude, the differences in fluid density were negligible (Akashi et al., 2000). We caution that use of other compounds such as methyl cellulose to increase water viscosity may produce a non-Newtonian fluid in which the forces generated depend on shear rate, making interpretation of changes in kinematics due to changes in viscosity challenging.

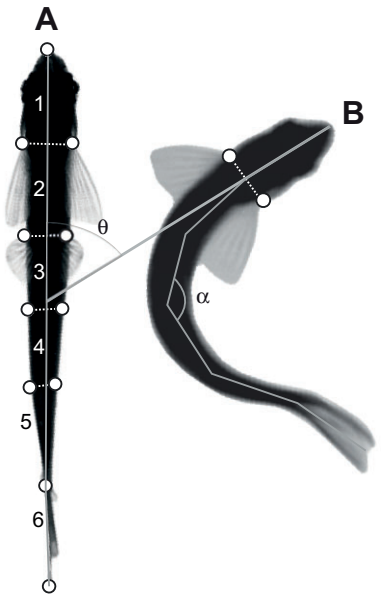

Fig. 1. Digitized points along the zebrafish body. The points marked with a white dot on the straight fish represent the digitized points in each frame. Points were chosen on either side of the body in order to facilitate reconstruction of the body midline. The body midline was split into six segments and the angle between these segments (α) was used as an estimate of localized body curvature. The instantaneous turn angle (θ) was defined as the angle through which the first midline body segment rotated from its original orientation (A) to the current image frame (B).

Viscosity manipulations have been used in a number of previous studies to separate the effects of temperature and viscosity on locomotor performance and to examine the hydrodynamics of behaviors at low Reynolds numbers. Here, we report viscosity in Pa s, the SI unit for dynamic (or absolute) viscosity. The viscosity values of 10 and 20 mPa s were chosen because we expected that viscosity levels 10 and 20 times the normal viscosity of water would be outside the natural range any fish would experience and hence would represent a significant challenge to fish performing escape responses at already maximal power outputs.

All experimental protocols were approved by Harvard University's institutional animal care and use committee.

Video analysis

At least three video sequences of escape responses were digitized in Matlab (The MathWorks Inc., Natick, MA, USA) for each individual at each viscosity using a custom-written program (Hedrick, 2008) for a total of 52 escape responses. Eleven points were digitized in each frame (Fig. 1): the tip of the snout, the base of each pectoral fin, the base of each pelvic fin, points on either side of the body 1/3 and 2/3 of the distance between the pelvic fin base and the caudal peduncle, the caudal peduncle and the tip of the dorsal caudal lobe. From these points a body midline was reconstructed in six segments and the angles between the segments were used to characterize body curvature.

The two stages of each escape response were identified as described by previous authors (e.g. Domenici and Blake, 1991; Tytell and Lauder, 2008). Stage 1 began in the frame of the first visible movement of the fish's snout and ended when angular

Table 1. Univariate ANOVA results for 25 kinematic variables during zebrafish C-starts

Variable	Viscosity	Individual	Viscosity×	Steady or unsteady	St1 or St2
Duration (ms): St1	0.59	0.64	0.18		St1
Duration (ms): St2	0.19	0.0003	0.0001*		St2
Maximum turn angle (deg)	0.26	0.74	0.56	Steady	St1
Maximum angular velocity (deg s^{-1})	<0.0001*,[1]	0.04	0.20	Steady	
Maximum angular acceleration (deg s^{-2})	0.018	0.57	0.23	Unsteady	
Final turn angle (deg)	0.11	0.79	0.51	Steady	St2
Maximum COM velocity (mm s^{-1})	<0.0001*,[2]	0.041	0.37	Steady	
Maximum tail velocity (mm s^{-1})	0.82	0.41	0.54	Steady	
St1 angle (deg)	0.26	0.58	0.35	Steady	St1
Maximum angular velocity in St1 (deg s^{-1})	<0.0001*,[1]	0.04	0.20	Steady	St1
Maximum angular acceleration in St1 (deg s^{-2})	0.0057*,[3]	0.32	0.04	Unsteady	St1
Maximum angular velocity in St2 (deg s^{-1})	0.0028*	0.27	0.25	Steady	St2
Maximum angular acceleration in St2 (deg s^{-2})	0.0018*,[1]	0.39	0.51	Unsteady	St2
COM displacement at St1 (mm)	<0.0003*,[1]	0.46	0.47	Steady	St1
COM displacement at St2 (mm)	0.0020	0.30	0.12	Steady	St2
COM displacement at 30 ms (mm)	0.0001*,[1]	0.16	0.72	Steady	
Time to maximum turn angle (ms)	0.27	0.67	0.05		
Time to maximum angular velocity (ms)	0.92	0.81	0.62	Unsteady	
Time to maximum angular acceleration (ms)	0.0061*,[3]	0.89	0.52		
Time to maximum COM velocity (ms)	0.0007*	0.71	0.14	Unsteady	
Time to maximum tail velocity (ms)	0.25	0.10	0.10	Unsteady	
Time to maximum angular velocity St1 (ms)	0.92	0.81	0.60	Unsteady	St1
Time to maximum angular acceleration St1 (ms)	0.026	0.90	0.96		St1
Time to maximum angular velocity St2 (ms)	0.61	0.15	0.15	Unsteady	St2
Time to maximum angular acceleration St2 (ms)	0.08	0.04	0.11		St2

Data are *P*-values (see Results for discussion). St1 and St2 refer to stage 1 and stage 2 of the C-start escape response; 'steady' refers to velocity-dependent variables; 'unsteady' refers to acceleration-dependent variables.

*Significant at 0.01 level.

[1]Mean value for water differed from both high viscosity treatments but the high viscosity means did not differ (Tukey HSD).

[2]Mean value for water and 10 mPa s were indistinguishable but different from the mean at 20 mPa s (Tukey HSD).

[3]Mean value for water was significantly different from the value at 10 mPa s but both were indistinguishable from the mean value at 20 mPa s.

velocity first returned to zero, indicating that the fish had stopped turning and had completed the initial C-bend [see Table 1; Duration (ms): St1]. Stage 2 ended when angular velocity returned to zero for the second time [Table 1; Duration (ms): St2].

For each video frame the turn angle, θ, was calculated. This was designated as the angle that the midline of the first body segment would make with the midline of this same segment in the first frame of the turn (Fig. 1). For each video sequence we then recorded the maximum turn angle, and the turn angle at the end of stage 1 and at the end of stage 2 (Table 1; St1 angle and final turn angle, respectively). Instantaneous angular velocity and acceleration were calculated by dividing turn angle changes by the time between consecutive image frames (1 ms). From these values, we recorded maximum angular velocity and acceleration for the entire escape response and for each stage of the turn (Table 1). Instantaneous linear displacement of the center of mass (COM) in a stretched-straight fish (see Jayne and Lauder, 1993; Tytell and Lauder, 2002) was calculated as the linear distance traveled by the midpoint between the pectoral fins (end of body segment 1) relative to its initial position. Displacement at the end of each stage as well as after a predetermined amount of time was then recorded for each swimming sequence (Table 1; COM displacement in St1, COM displacement in St2, COM displacement at 30 ms). Linear velocity and acceleration were calculated by dividing displacement by the time between consecutive image frames. The process was repeated for displacement and velocity of the tail (Fig. 1). We then recorded the maximum linear velocity of the COM and of the tail (Table 1). For all maxima calculated, we also recorded the time it took for the maximum to be reached from the beginning of the escape response (e.g. time to maximum turn angle; Table 1).

Statistics

To determine whether there was an overall viscosity effect, we performed three multivariate analyses of the dataset. First, the dataset was analyzed using a multivariate ANOVA with viscosity as a fixed effect and 21 kinematic response variables (Table 1). Maximum velocity and acceleration and the time to these values were not included in these analyses because they also appeared in the dataset as the maximum values in either stage 1 or stage 2. A significant multivariate ANOVA result for viscosity was then followed by *post hoc* univariate ANOVA on each of the kinematic variables with viscosity as a fixed effect and individual fish as a random factor (Zar, 1999). The results of the univariate ANOVA were deemed significant if supported by a *P*-value smaller than 0.01 (Table 1); this stringent significance level was chosen to reduce the chance of false null hypothesis rejections due to multiple comparisons.

Second, a discriminant function analysis using the same 21 variables was then conducted to determine whether it was possible to correctly classify individual escape responses by their viscosity. Third, to further investigate the possible differential effect of viscosity treatment on stage 1 and 2 of the escape response and the effects of body acceleration, kinematic variables were categorized as contributing to steady or unsteady hydrodynamics, and as belonging to either stage 1 or stage 2 (see Table 1). For each class of variables a principal components analysis was run followed by a MANOVA on the first four principal components. All statistics were calculated in JMP (version 9, SAS Institute Inc., Cary, NC, USA).

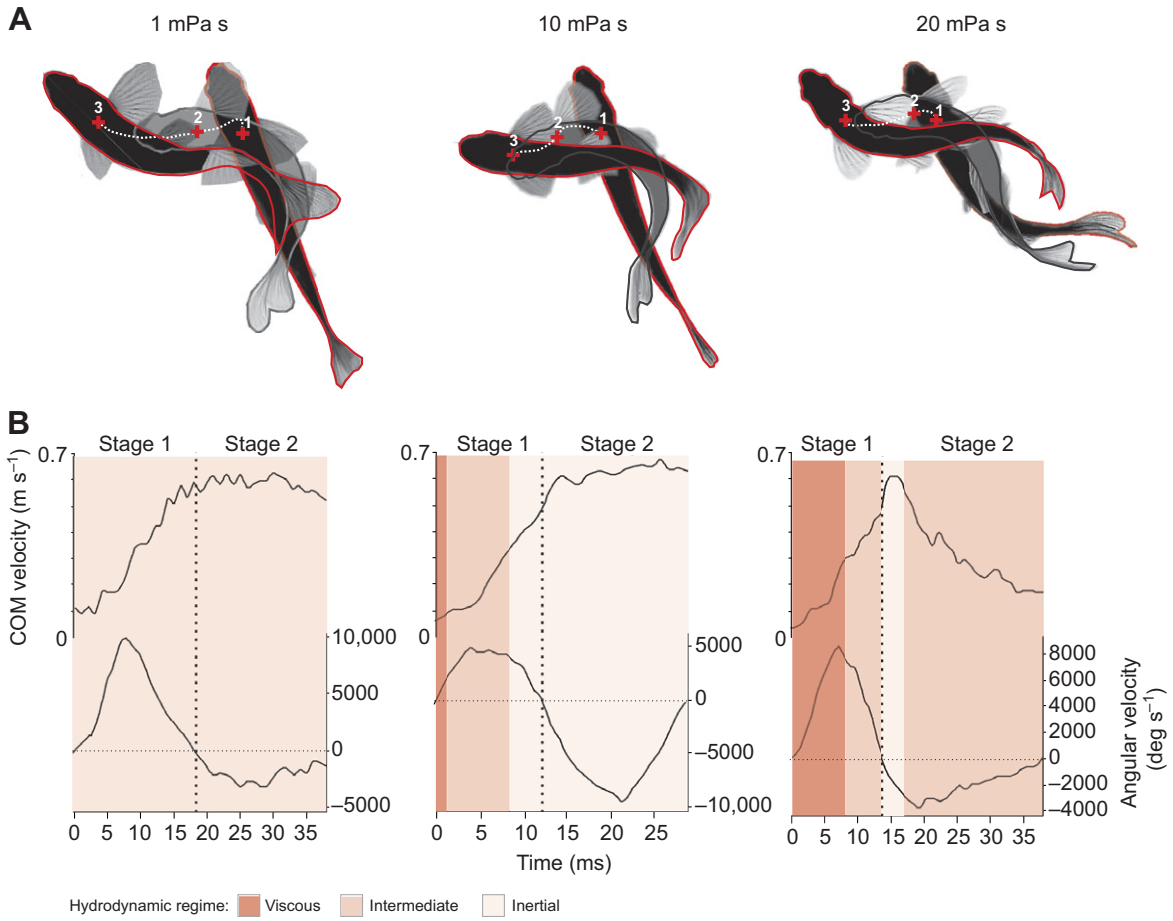

Fig. 2. A sample C-start escape from each viscosity treatment. These three sequences were mechanically initiated and are from the same individual. (A) Images of fish outlines and estimated center of mass (COM) for the stretched-straight fish at the start, the end of stage 1, and the end of stage 2. The dotted white line follows the COM path. (B) Instantaneous velocity of the COM and instantaneous angular velocity of the head. The hydrodynamic regimes are colored such that Re<300 indicates viscous conditions, 300<Re<1000 intermediate and Re>1000 the inertial regime following McHenry and Lauder (McHenry and Lauder, 2005). Linear velocity dropped significantly more between the end of stage 1 and the end of stage 2 in the high viscosity water compared with normal water.

RESULTS

Fifty-two escape responses were studied from 5 fish. Thirty-one of the turns were initiated after the dropped object impacted the surface of the water; these we called mechanically stimulated turns. Twenty-one of the turns began before the object hit the surface of the water; these we called visually stimulated turns. Mechanically stimulated turns constituted 71% of the escape turns in normal water (1 mPa s), 50% in 10 mPa s and 59% in 20 mPa s. The observed viscosity effects could be due to an alteration of the physics of mechanosensation (McHenry et al., 2009a). Therefore, for mechanically stimulated turns we also measured the time between the stimulus and the first frame of the turn (latency), the angle between the dorsal midline of the fish and a line connecting the center of mass of the fish to the stimulus location (angle to stimulus at turn start) as well as the linear distance between the fish center of mass at the beginning and end of the stimulus (distance to stimulus). Neither viscosity nor individual had any significant effect on the variables, although there was a tendency for latency to be shorter in higher viscosity media. We therefore grouped all C-starts together for subsequent analyses.

Reynolds number calculations using fish length, maximum linear velocity per sequence and the appropriate viscosity for each treatment show our manipulations altered the maximum Reynolds number of a sequence by an order of magnitude between consecutive viscosity levels. The mean maximum Reynolds number in 1 mPa s water was 27,800 (±2140 s.e.m.) compared with 2350 (±160 s.e.m.) and 820 (±60 s.e.m.) in 10 and 20 mPa s fluid, respectively. Fish escaping in normal water (1 mPa s) operated in the inertial hydrodynamic regime for the entire duration of the escape response (Fig. 2B). The effect of viscosity became apparent at 10 mPa s viscosity, where the initial angular acceleration took place under viscous hydrodynamic conditions, proceeded past the point of maximum angular velocity in an intermediate regime and ended with high linear velocity and constant angular acceleration in the inertial regime (Fig. 2B). Fish performing escape responses in the highest viscosity treatment, 20 mPa s, spent a very small proportion of the turn in the inertial regime, while most of the turn was under the complex hydrodynamics of the intermediate regime (Fig. 2B).

Escape responses at all viscosities followed the same general sequence of characteristic behavioral events typical of a fish C-start in normal water. Fig. 2 provides an example of a typical C-start from the same fish at each of the three viscosities tested. Each C-start shows the characteristic stage 1 and stage 2 components. The duration of each stage did not show a significant viscosity effect (Fig. 3; Table 1). Although the angular velocity profiles are similar

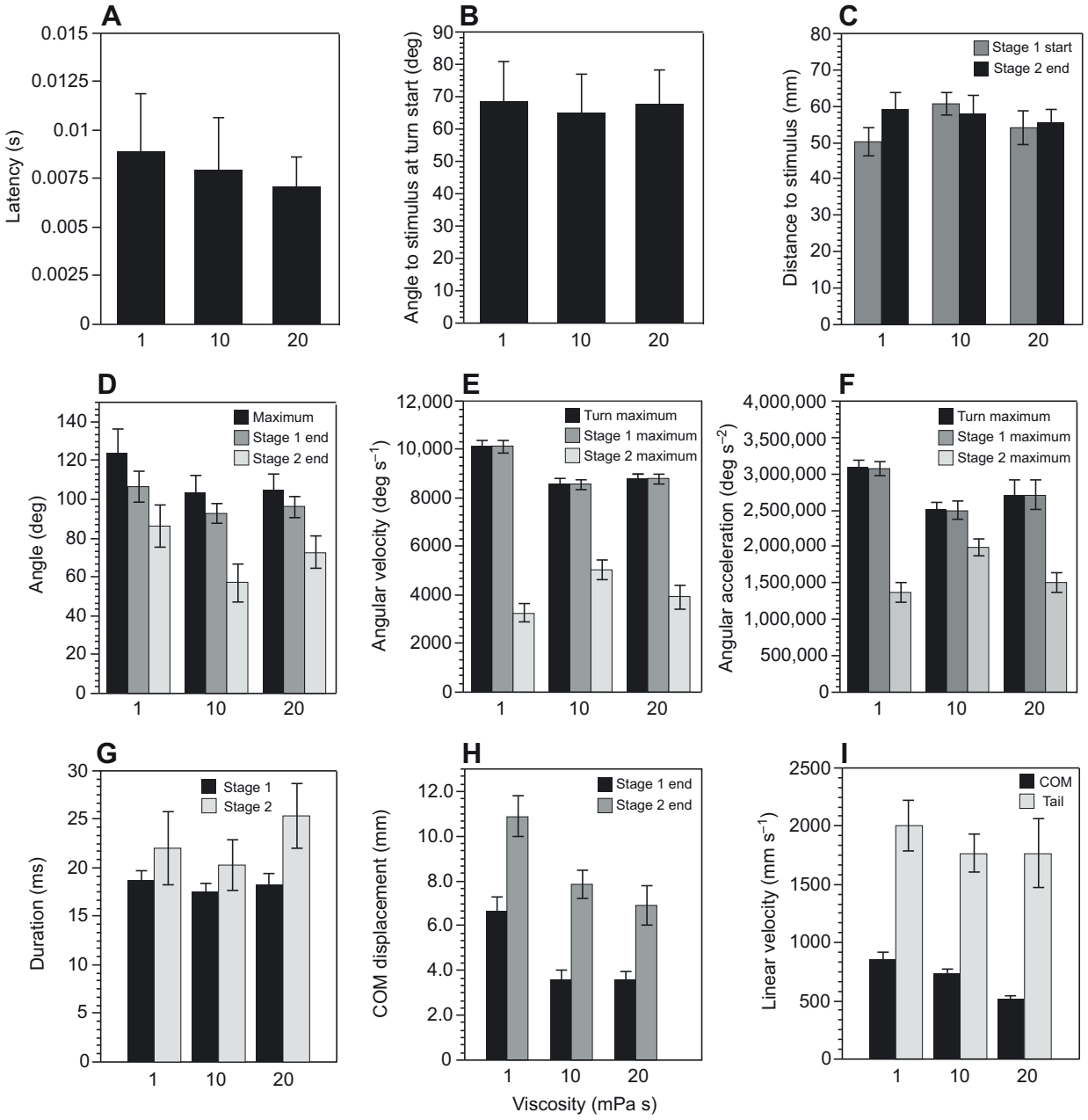

Fig. 3. Selected kinematic variables (means + s.e.m.) at each viscosity treatment separated into stage 1 and stage 2 where appropriate. A–C summarize kinematic variables specific to mechanically stimulated turns; D–F show angular variables; G–I show duration, linear displacement and velocity of C-starts. See Table 1 for statistical results.

for all viscosities, linear velocity dropped sharply by the end of stage 2 in the highest viscosity treatment (Fig. 2B). The reduction in linear velocity during stage 2 was significantly higher at 20 mPa s viscosity compared to turns in water (Tukey's HSD). In general, linear velocities at the end of stage 1 as well as the maximum velocity reached during that stage were significantly higher in water than in both increased viscosity treatments (Tukey's HSD; Fig. 3).

As shown in Table 1, only 10 kinematic variables had a significant viscosity effect: maximum angular velocity, maximum COM velocity, maximum angular velocity and acceleration in both stages, COM displacement at the end of stage 1 and after 30 ms, time to maximum angular acceleration and time to maximum COM velocity. No variable showed an effect of individual, although the duration of stage 2 had a significant viscosity by individual effect (Table 1). *Post hoc* tests (Tukey HSD) indicated that the mean kinematic value never differed among all three viscosities (Table 1). Instead, two of the viscosities grouped together but differed from the third, or two viscosities were significantly different from each other but both were indistinguishable from the third (Table 1).

Maximum turn angles during the escape responses occurred in stage 2 while maximum angular velocity and acceleration both occurred during stage 1 (Fig. 3). Stage 1 angle correlated significantly with stage 2 angle in all viscosities (R^2=0.80, regression slope=1.2, P<0.0001 in 1 mPa s water; R^2=0.52, regression slope=1.4, P=0.0007 in 10 mPa s fluid; and R^2=0.44, regression slope=1.0, P=0.0036 in 20 mPa s fluid).

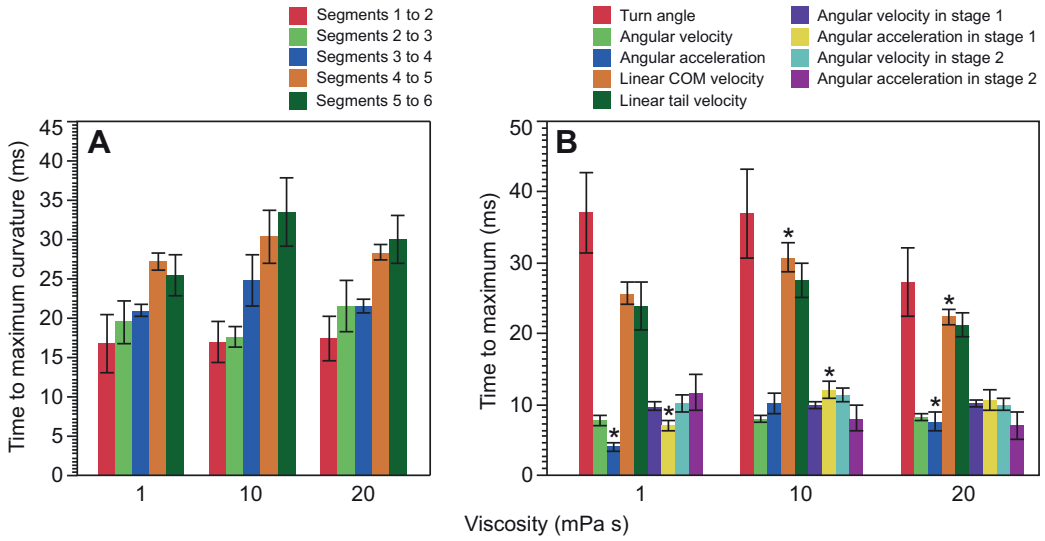

Fig. 4. (A) Time to maximum angle measured between adjacent body segments. In all viscosities, maximum body bending proceeded anteroposteriorly without any significant differences among the viscosity treatments in time to maximum body curvature at any body location. (B) Time to maximum for a selection of kinematic variables. Maximum angular velocity and acceleration in stage 1 are also the maximum values achieved during the entire escape response. Each bar represents the mean of all escape responses in each viscosity; error bars are s.e.m. See Table 1 for statistical results.

In all viscosities, maximum body bending proceeded anteroposteriorly without any significant differences among the viscosity treatments (Fig. 4A). The time to maximum angular acceleration and time to maximum COM velocity were significantly affected by the viscosity treatments (Fig. 4B; Table 1).

Univariate ANOVA tests were carried out for all 25 kinematic variables common to both visually and mechanically stimulated turns, as the overall MANOVA on the viscosity effect was significant (Wilk's lambda, P=0.0006). MANOVA of the first four principal components for the data set separated by each *a priori* kinematic category (steady, unsteady, stage 1 and stage 2) were all significant (Wilk's lambda, P<0.0001, 0.0034, 0.0002 and 0.0048, respectively), indicating that changing viscosity had a significant overall effect on each stage as well as on variables separated by proposed locomotor pattern.

The discriminant function analysis was able to correctly categorize 94% of the escape responses based on the 21 kinematic variables used (Fig. 5). The first two canonical functions explained 100% of the variation (83.5% and 16.5%, respectively). The variables with the two highest positive and the two lowest negative coefficients for canonical 1 were the following: linear displacement of the COM after 30 ms (4.88), linear displacement of the COM at the end of stage 2 (0.31), stage 1 duration (–0.50) and time to maximum angular velocity in stage 1 (–0.16). The variables with the two highest and two lowest coefficients for canonical 2 were: time to maximum turn angle (0.29), linear displacement of the COM at the end of stage 2 (0.11), linear displacement of the COM after 30 ms (–1.04) and time to maximum angular velocity in stage 1 (0.20).

DISCUSSION

In this paper, we explored the influence of viscosity on C-start escape behaviors by studying the response of a classic high-speed behavior to substantial changes in the external medium. Our multivariate statistical analyses show a statistically significant overall effect of viscosity, indicating that fish displayed altered kinematics as the viscosity of water was increased to 10 and 20 times that of normal water. And the discriminant function analysis showed that 94% of the C-starts could be correctly classified using the kinematic variables that we extracted from the escape responses. We expected *a priori* that duration and timing variables would show an increase in magnitude as viscosity increased and that there might be differences in how kinematic variables that reflect velocity responded to viscosity changes compared with those variables that reflect body accelerations.

Thus, we were surprised to find that variables such as the duration of stage 1 and stage 2 did not show a viscosity effect and that several other variables such as final turn angle and maximal turn angle, and the time to reach many of the maximal velocity and acceleration variables were also not affected by viscosity (Table 1). In addition, the finding that variables such as maximum angular acceleration and the timing of some acceleration maxima did not differ in the increased viscosity treatments was unexpected.

Nonetheless, increasing water viscosity did have several significant effects on escape kinematics and did not have the same effect on all aspects of the C-start. Whereas normal escape responses happened exclusively in the inertial regime based on Reynolds number calculations throughout the escape response (Fig. 2B), a significant proportion of escape responses in high viscosity occurred either in the viscous or the intermediate regimes. The Reynolds number (the ratio of inertial to viscous forces) cut-off points for these regimes in the zebrafish *D. rerio* were shown experimentally

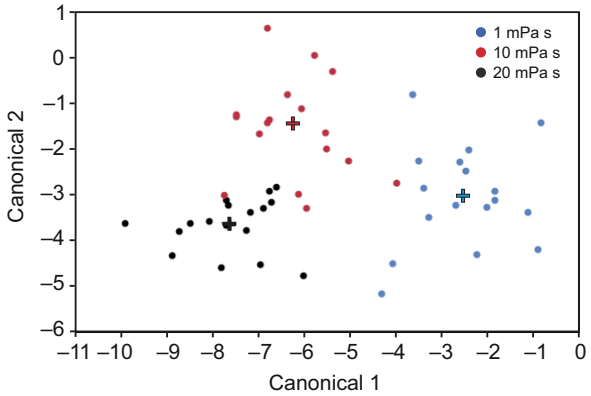

Fig. 5. Discriminant function analysis showing that swimming medium could be correctly identified for 94% of the turns based on escape response kinematics. Crosses represent the mean scores for each viscosity. All the variables presented in Table 1 were used, except for maximum angular velocity and acceleration, and the times to these variables (total of 21 variables).

to be 300 for the upper end of the viscous regime and 1000 for the lower end of the inertial regime (McHenry and Lauder, 2005). In the viscous regime, motion should be dominated by water viscosity, body length and velocity. In contrast, motion in the inertial regime is affected by the water density, the wetted surface area of the fish body and the square of velocity (Vogel, 1994).

Escape responses in 10 times the viscosity of water only reached the inertial regime 75% into the duration of stage 1 (Fig. 2B), with approximately the first 10% of this stage under viscous conditions and the remaining 65% under intermediate hydrodynamic conditions. At 20 mPa s, only a small fraction (~10%) of the turn occurred under dominantly inertial forces while the majority of the turn was performed in the intermediate hydrodynamic regime (Fig. 2B).

Evaluating hypotheses of viscosity effects

Escape responses are vital to a fish's survival. For this reason, fish muscles are likely to operate near their limits for producing power during these brief events, and this view has been commonly argued in the literature (e.g. Franklin and Johnston, 1997; Johnston et al., 1995; Wakeling and Johnston, 1998). Consequently, we expected that an increase in fluid viscosity would result in slower escape responses. However, the duration of each stage and hence of the whole turn did not change in high viscosity (Table 1, Fig. 3G), hinting at similar timings of hydrodynamic force generation during stage 1 and 2 and for a limited effect on the hydrodynamics of fin function (Tytell and Lauder, 2008). This result also suggests that the duration of neuromuscular stimulation was unchanged despite the novel hydrodynamic environments, a finding in concert with the low amount of variation previously observed for this stage in normal water (Domenici and Blake, 1991; Tytell and Lauder, 2008). If higher viscosity environments require increased muscle power production for motions of the same duration, then myomeres may develop increased power production through an increase in stimulation frequency, or through increased muscle fiber recruitment. This may be true even if myotomal musculature is activated for similar durations in all viscosities. It is not currently known whether all myotomal muscle fibers are activated maximally during a zebrafish C-start escape behavior, but changes in activation of different regions of myotomes have been documented for other locomotor behaviors in other species (Jayne and Lauder, 1995). Models of myotomal muscle function commonly assume that all fibers within each myotomal segment are activated completely during behaviors that require white myotomal fiber recruitment, but increased power production could be achieved through recruitment of additional fibers not normally activated even during the C-start behavior, commonly believed to be a maximal behavior in normal viscosity water.

When Mauthner cells activating the escape response in fishes are directly stimulated, stage 1 duration and angle are constant (Wakeling, 2006) and both directly correlate with the duration of muscle activity in stage 1 (Eaton et al., 1988). Stage 2 angle (final angle in this study) has been shown to correlate with stage 1 angle, giving rise to the term 'ballistic' to describe the neural command of this behavior (Eaton and Emberley, 1991), as initiation of the turn by the Mauthner cells controls the amount of body bending and as a consequence the final angle of an escape turn. However, stage 2 angle responded differently from stage 1 angle to changing viscosity in our experiments, and also was not linearly related to viscosity: stage 2 angle decreased more in 10 mPa s fluid than it did in 20 mPa s fluid, while stage 1 angle decreased by the same amount in both high viscosity treatments (Fig. 3D). Stage 1 and 2 angles were also uncorrelated in a study of larval zebrafish raised in high viscosity environments (Danos, 2012).

Swimming kinematics are ultimately a product of the interaction between the fluid, the fish body and the contractile properties of the underlying musculature. An interesting simulation study recently demonstrated the effect of viscosity on lamprey swimming kinematics (Tytell et al., 2010). By keeping all parameters of the simulation constant, including neuromuscular input and body stiffness, but increasing viscosity to 10 times that of water (10 mPa s), the authors were able to observe the following kinematic changes in simulated swimming: a 50% reduction in swimming speed and initial acceleration, and an order of magnitude increase in the relative amount of muscle power required to swim at a steady speed (Tytell et al., 2010). Although the effect of viscosity on linear velocity is not nearly as pronounced in real fish performing escape turns, there is a significant effect of viscosity on maximum linear velocity and displacement of the center of mass (Table 1). This indicates that even under the unsteady and high Reynolds conditions of a fast-starting fish, viscous forces play a significant role.

Using viscosity as an environmental manipulation

The manipulation of water viscosity is a powerful tool to assist in the dissection of organismal biomechanics, and a number of studies have applied this approach on a wide range of organisms. In Table 2 we summarize a selection of recent studies manipulating viscosity and add notes on the specific viscous agent used and selected information on some of the conclusions drawn.

There are a variety of possible agents that could be added to water to increase viscosity, but we believe it is important to emphasize that for studies that involve rapid motion, a Newtonian agent such as Dextran should be used. The shear thinning that results from rapid motion in a non-Newtonian fluid could certainly affect results, and undermine attempts to maintain a constant treatment viscosity effect when motions differing in acceleration are studied.

A number of the studies mentioned in Table 2 have used viscosity manipulations to compensate for changes in water properties as temperature is altered. Temperature can have dramatic effects on organismal function and it is often useful to quantify these effects by calculating Q_{10} (e.g. Podolsky and Emlet, 1993). However, a 10°C increase in the temperature of water from 10°C to 20°C also causes a 23% decrease in both dynamic and kinematic viscosity. Kinematic viscosity decreases slightly faster than dynamic viscosity (e.g. 23.18% compared with 23.33% in the example above) and hence studies that use viscosity manipulations while testing for the effects of temperature tend to report kinematic viscosity ($m^2 s^{-1}$). Within the range of natural temperature and viscosity fluctuations, most studies found that the physiological effects of temperature far outweighed any physical effects of viscosity, except for organisms of very small sizes such as bacteria operating at extremely low Reynolds numbers (Beveridge et al., 2010).

In this study, we used a viscosity manipulation to show that fishes, even when challenged with a 20-fold increase in water viscosity, are able to perform escape behaviors of similar duration and stage 1 angle to those executed in normal water. We did observe several specific alterations in escape kinematics and multivariate analysis confirms a significant overall viscosity effect, although the effects were not along the predicted lines of steady *versus* unsteady kinematics. Our results therefore suggest that fishes may be able to generate greater muscular power than has been suspected when confronted with a more viscous medium, and that activations of myotomal musculature in normal water, even for the C-start, may not be maximal. Alternatively, the complex hydrodynamics of the

Table 2. Summary of selected studies that have used viscosity manipulations to study organismal movement

Study	Viscous agent	Kinematic viscosity ($m^2\ s^{-1}$)	Dynamic viscosity (Pa s)	Notes
Beveridge et al., 2010	Ficoll	1×10^{-6} to 1.5×10^{-6}		Temperature-dependent viscosity had a significant effect on the carrying capacity and growth rates of consumers (bacteria), as well as the average density of the top predator (ciliates).
Horner and Jayne, 2008	Poly-Bore	10, 100 and 1000		Shear-thinning, non-Newtonian thickening agent used to study lungfish locomotion in mud-like conditions. Lungfish did not switch to a terrestrial motor pattern at high viscosity.
Hubley et al., 2001	Ficoll	4% (w/v)		Distinguished the effects of temperature and viscosity on the locomotor capacity of juvenile annelid polychaetes. Found no effect of viscosity.
Hunt von Herbing and Keating, 2003	Methyl cellulose	1.32×10^{-6} to 2.2×10^{-6}		Decreasing viscosity effects and increasing physiological effects of temperature on swimming performance with increasing size of larval Atlantic haddock.
Johnson et al., 1998	Dextran (M_r 242,000)	1, 1.6 and 3.4		Reduction in temperature from 20 to 5°C also causes a 1.6-fold increase in viscosity. However, there was little effect of viscosity on C-start kinematics even for a small fish like *Poecilia*.
Korta et al., 2007	Methyl cellulose		0.05–50	Swimming gait of *C. elegans* does not vary across the range of viscosities but the temporal frequency of the swimming gait decreases by ~20% with every 10-fold increase in viscosity.
Podolsky and Emlet, 1993	Polivinyl pyrrolidone		1.02×10^{-3} to 1.3×10^{-3}	Calculated Q_{10} for sand dollar larvae by factoring in viscosity effects.
Pate and Brokaw, 1980	Ficoll		1.1×10^{-3} to 8×10^{-3}	Compared locomotor effects of ficoll to methyl cellulose study in sea urchin spermatozoa. Found reduced beat frequency in higher viscosity.
McHenry and Lauder, 2005	Dextran		1.2×10^{-3} to 18×10^{-3}	Coasting and drag over zebrafish ontogeny. Used viscosity to modify Reynolds number and its effect on drag coefficients.
Kanou et al., 2007	Methyl cellulose		32, 364 and 1344	The relative occurrence of walking in the insect *Gryllus bimaculatus* increased with viscosity suggesting that a reacting force from the substrate to the legs is one of the factors important in triggering walking.
Neugebauer et al., 1998;	Percoll		Up to 1.5×10^{-3}	Central and peripheral graviperception in ciliates.
Jordan, 1998	Poly-Ox		Up to 0.06	Scale effects in the kinematics and dynamics of swimming leeches. Significant kinematic changes in high viscosity.

intermediate hydrodynamic regime in which a large proportion of the observed escape responses occurred may lead to an even more complex muscle–fluid interaction. Such an interaction may lead to changes in the timing of hydrodynamic force production interplay with the muscle's intrinsic force–velocity properties.

Sensory input and viscosity

The role of sensory input during rapid fish behaviors such as the escape response is still a topic of active investigation, and there are several possible views of how sensory systems could modulate escape kinematics. On the one hand, there is a high correlation of stage 1 and stage 2 angles in escaping fish under normal viscosity conditions, suggesting a ballistic-type neural control of escape that is independent of sensory information gathered during the initial stages of the turn. On the other hand, there is a high degree of consistency in stage 1 angles of zebrafish larvae C-starts despite substantial differences in water viscosity (Danos, 2012), and the use of prey position information in predicting the kinematics of archer fish predatory attacks (Wohl and Schuster, 2007). Archer fish shoot insects out of trees with a bolus of water and then use escape response kinematics to move to the location where they predict the insect will fall on the water surface (Wohl and Schuster, 2006; Wohl and Schuster, 2007). The fact that archer fish can integrate sensory information with escape response kinematics suggests that not all neural control pathways of this behavior are deterministic.

Interesting recent work (McHenry et al., 2009a; Windsor and McHenry, 2009) has begun to examine the interaction between the mechanical properties of neuromasts and hydrodynamics. When quantifying the time between the impact of a dropped object onto the water surface and the first movement of the fish's head (latency), we found a tendency (though non-significant) for latency to decrease as viscosity increases (Fig. 3A). Larval zebrafish had a latency of 13–15 ms when stimulated with a uniform flow field (McHenry et al., 2009b), while the mean latency of the adult zebrafish in this study was 8.9 ms in normal water, 8 ms in 10 mPa s fluid and 7.1 ms in 20 mPa s fluid. The tendency towards increased sensitivity at high viscosity likely represents the increased drag acting on superficial neuromasts resulting in increased wall shear stress around the superficial neuromasts, similar to the increase in sensitivity observed when the effective cross-sectional area of artificial neuromasts is increased (Peleshanko et al., 2007; Windsor and McHenry, 2009). Analysis of the role of fish sensory systems in modulating rapid behaviors such as C-starts is an interesting area for future investigation.

ACKNOWLEDGEMENTS

We are grateful to Johannes Oeffner for assistance with data collection and to Christopher Richards for constructive comments on the manuscript.

FUNDING

This research was supported by the National Science Foundation (NSF) [grant no. EFRI-0938043 to G.L.].

REFERENCES

Akashi, N., Kushibiki, J.-I. and Dunn, F. (2000). Measurements of acoustic properties of aqueous dextran solutions in the VHF/UHF range. *Ultrasonics* **38**, 915-919.

Beveridge, O. S., Petchey, O. L. and Humphries, S. (2010). Direct and indirect effects of temperature on the population dynamics and ecosystem functioning of aquatic microbial ecosystems. *J. Anim. Ecol.* **79**, 1324-1331.

Borazjani, I., Sotiropoulos, F., Tytell, E. D. and Lauder, G. V. (2012). On the hydrodynamics of the bluegill sunfish C-start escape response: three-dimensional simulations and comparison with experimental data. *J. Exp. Biol.* **215**, 671-684.

Daniel, T. L. (1984). Unsteady aspects of aquatic locomotion. *Am. Zool.* **24**, 121-134.

Danos, N. (2012). Locomotor development of zebrafish (*Danio rerio*) under novel hydrodynamic conditions. *J. Exp. Zool. A* (in press).

Domenici, P. and Blake, R. W. (1991). The kinematics and performance of the escape response in the angelfish (*Pterophyllum eimekei*). *J. Exp. Biol.* **156**, 187-205.

Domenici, P. and Blake, R. W. (1997). The kinematics and performance of fish fast-start swimming. *J. Exp. Biol.* **200**, 1165-1178.

Drucker, E. G. and Lauder, G. V. (2005). Locomotor function of the dorsal fin in rainbow trout: kinematic patterns and hydrodynamic forces. *J. Exp. Biol.* **208**, 4479-4494.

Eaton, R., Bombardieri, R. and Meyer, D. (1977). The Mauthner-initiated startle response in teleost fish. *J. Exp. Biol.* **66**, 65-81.

Eaton, R. C. and Emberley, D. S. (1991). How stimulus direction determines the trajectory of the Mauthner-initiated escape response in a teleost fish. *J. Exp. Biol.* **161**, 469-487.

Eaton, R. C., Didomenico, R. and Nissanov, J. (1988). Flexible body dynamics of goldfish c-start – implications for reticulospinal command mechanisms. *J. Neurosci.* **8**, 2758-2768.

Faber, T. E. (1995). *Fluid Dynamics for Physicists*. Cambridge: Cambridge University Press.

Foreman, M. B. and Eaton, R. C. (1993). The direction change concept for reticulospinal control of goldfish escape. *J. Neurosci.* **13**, 4101-4113.

Franklin, C. and Johnston, I. (1997). Muscle power output during escape responses in an Antarctic fish. *J. Exp. Biol.* **200**, 703-712.

Frith, H. R. and Blake, R. W. (1995). The mechanical power output and hydromechanical efficiency of northern pike (*Esox lucius*) fast-starts. *J. Exp. Biol.* **198**, 1863-1873.

Hedrick, T. L. (2008). Software techniques for two- and three-dimensional kinematic measurements of biological and biomimetic systems. *Bioinspir. Biomim.* **3**, 034001.

Horner, A. M. and Jayne, B. C. (2008). The effects of viscosity on the axial motor pattern and kinematics of the African lungfish (*Protopterus annectens*) during lateral undulatory swimming. *J. Exp. Biol.* **211**, 1612-1622.

Hubley, M. J., Parks, C. D. A. and Lin, J. (2001). Temperature-induced changes in the locomotor capacity of juveniles of *Marenzelleria viridis* (Polychaeta, Spionidae). *Invert. Biol.* **120**, 372-377.

Hunt von Herbing, I. and Keating, K. (2003). Temperature-induced changes in viscosity and its effects on swimming speed in larval haddock. In *The Big Fish Bang.* Proceedings of the 26th Annual Larval Fish Conference, 2003 (ed. H. I. Browman and A. Berit Skiftesvik), pp. 23-34. Bergen, Norway.

Jayne, B. C. and Lauder, G. V. (1993). Red and white muscle activity and kinematics of the escape response of the bluegill sunfish during swimming. *J. Comp. Physiol. A* **173**, 495-508.

Jayne, B. C. and Lauder, G. V. (1995). Are muscle fibers within fish myotomes activated synchronously? Patterns of recruitment within deep myomeric musculature during swimming in largemouth bass. *J. Exp. Biol.* **198**, 805-815.

Johnston, I. A., Van Leeuwen, J., Davies, M. and Beddow, T. (1995). How fish power predation fast-starts. *J. Exp. Biol.* **198**, 1851-1861.

Johnson, T. P., Cullum, A. J. and Bennett, A. F. (1998). Partitioning the effects of temperature and kinematic viscosity on the C-start performance of adult fishes. *J. Exp. Biol.* **201**, 2045-2051.

Jordan, C. E. (1998). Scale effects in the kinematics and dynamics of swimming leeches. *Can. J. Zool.* **76**, 1869-1877.

Kanou, M., Morita, S., Matsuura, T. and Yamaguchi, T. (2007). Analysis of behavioral selection after sensory deprivation of legs in the cricket *Gryllus bimaculatus*. *Zoolog. Sci.* **24**, 945-952.

Korta, J., Clark, D. A., Gabel, C. V., Mahadevan, L. and Samuel, A. D. T. (2007). Mechanosensation and mechanical load modulate the locomotory gait of swimming *C. elegans*. *J. Exp. Biol.* **210**, 2383-2389.

Liu, K. S. and Fetcho, J. R. (1999). Laser ablations reveal functional relationships of segmental hindbrain neurons in zebrafish. *Neuron* **23**, 325-335.

McHenry, M. J. and Lauder, G. V. (2005). The mechanical scaling of coasting in zebrafish (*Danio rerio*). *J. Exp. Biol.* **208**, 2289-2301.

McHenry, M. J., Strother, J. A. and Van Trump, W. J. (2009a). Fluid-structure interaction in lateral line receptors. *Integr. Comp. Biol.* **49**, E113.

McHenry, M. J., Feitl, K. E., Strother, J. A. and Van Trump, W. J. (2009b). Larval zebrafish rapidly sense the water flow of a predator's strike. *Biol. Lett.* **5**, 477-479.

Neugebauer, D. C., Machemer-Rohnisch, S., Nagel, U., Braucker, R. and Machemer, H. (1998). Evidence of central and peripheral gravireception in the ciliate *Loxodes striatus*. *J. Comp. Physiol. A* **183**, 303-311.

Pate, E. F. and Brokaw, C. J. (1980). Movement of spermatozoa in viscous environments. *J. Exp. Biol.* **88**, 395-397.

Peleshanko, S., Julian, M. D., Ornatska, M., McConney, M. E., LeMieux, M. C., Chen, N., Tucker, C., Yang, Y., Liu, C., Humphrey, J. A. C. et al. (2007). Hydrogel-encapsulated microfabricated haircells mimicking fish cupula neuromast. *Adv. Mat.* **19**, 2903-2909.

Podolsky, R. D. and Emlet, R. B. (1993). Separating the effects of temperature and viscosity on swimming and water movement by sand dollar larvae (*Dendraster excentricus*). *J. Exp. Biol.* **176**, 207-221.

Rome, L. C., Funke, R. P., Alexander, R. M., Lutz, G., Aldridge, H., Scott, F. and Freadman, M. (1988). Why animals have different muscle-fiber types. *Nature* **335**, 824-827.

Standen, E. M. and Lauder, G. V. (2005). Dorsal and anal fin function in bluegill sunfish *Lepomis macrochirus*: three-dimensional kinematics during propulsion and maneuvering. *J. Exp. Biol.* **208**, 2753-2763.

Standen, E. M. and Lauder, G. V. (2007). Hydrodynamic function of dorsal and anal fins in brook trout (*Salvelinus fontinalis*). *J. Exp. Biol.* **210**, 325-339.

Tytell, E. D. and Lauder, G. V. (2002). The C-start escape response of *Polypterus senegalus*: bilateral muscle activity and variation during stage 1 and 2. *J. Exp. Biol.* **205**, 2591-2603.

Tytell, E. D. and Lauder, G. V. (2008). Hydrodynamics of the escape response in bluegill sunfish, *Lepomis macrochirus*. *J. Exp. Biol.* **211**, 3359-3369.

Tytell, E. D., Hsu, C.-Y., Williams, T. L., Cohen, A. H. and Fauci, L. J. (2010). Interactions between internal forces, body stiffness, and fluid environment in a neuromechanical model of lamprey swimming. *Proc. Natl. Acad. Sci. USA* **107**, 19832-19837.

Vogel, S. (1994). *Life in Moving Fluids: The Physical Biology of Flow*, 2nd edn. Princeton: Princeton University Press.

Wakeling, J. M. (2006). Fast-start mechanics. In *Fish Biomechanics*, Vol. 23, *Fish Physiology* (ed. R. E. Shadwick and G. V. Lauder), pp. 333-368. San Diego: Academic Press.

Wakeling, J. M. and Johnston, I. A. (1998). Muscle power output limits fast-start performance in fish. *J. Exp. Biol.* **201**, 1505-1526.

Walker, J. A., Ghalambor, C. K., Griset, O. L., McKenney, D. and Reznick, D. N. (2005). Do faster starts increase the probability of evading predators? *Funct. Ecol.* **19**, 808-815.

Weiss, S. A., Zottoli, S. J., Do, S. C., Faber, D. S. and Preuss, T. (2006). Correlation of C-start behaviors with neural activity recorded from the hindbrain in free-swimming goldfish (*Carassius auratus*). *J. Exp. Biol.* **209**, 4788-4801.

Westneat, M. W., Hale, M. E., McHenry, M. J. and Long, J. H. (1998). Mechanics of the fast-start: muscle function and the role of intramuscular pressure in the escape behavior of *Amia calva* and *Polypterus palmas*. *J. Exp. Biol.* **201**, 3041-3055.

Windsor, S. P. and McHenry, M. J. (2009). The influence of viscous hydrodynamics on the fish lateral-line system. *Integr. Comp. Biol.* **49**, 691-701.

Wohl, S. and Schuster, S. (2006). Hunting archer fish match their take-off speed to distance from the future point of catch. *J. Exp. Biol.* **209**, 141-151.

Wohl, S. and Schuster, S. (2007). The predictive start of hunting archer fish: a flexible and precise motor pattern performed with the kinematics of an escape C-start. *J. Exp. Biol.* **210**, 311-324.

Zar, J. H. (1999). *Biostatistical Analysis*. Upper Saddle River, NJ: Prentice Hall.

Zottoli, S. J. (1977). Correlation of startle reflex and Mauthner cell auditory responses in unrestrained goldfish. *J. Exp. Biol.* **66**, 243-254.